Chapter VI

Theoretical Estimation of Structural Parameters of Twist Grain Boundary -A Liquid Crystals

6.1 Introduction

In the previous chapter we have described some experimental studies on twist grain boundary liquid crystals. In this chapter we will theoretically estimate the structural parameters, namely the distance between two dislocations (l_d) within a grain boundary and that between two neighboring grain boundaries (l_b) in TGB_A liquid crystals.

In contrast to the Abrikosov lattice of flux tubes in type-II superconductors, a triangular lattice of screw dislocations which are *parallel in the direct lattice* of the SmA does not lead to a tenable structure [1]. Renn and Lubensky estimated the lower critical chiral strength (the analogue of the lower critical magnetic field in superconductors) by comparing the energy gained by twisting the structure to the energy cost of creating a *single* screw dislocation. This analysis is based on the surmise that inter-dislocation spacing near the lower critical chiral strength is very large compared to the twist penetration depth. In the extreme type–II limit (Ginzburg parameter $\kappa_2 >> 1/\sqrt{2}$) the lower critical strength $h_{c1} = (dD/4\pi)\ln(\lambda_2/\xi)$, where D is the coefficient of the covariant term in the elastic free energy (see equation.(5.5)), $\lambda_2^2 = K_2/D$, and d is the magnitude of the Burgers vector of the screw dislocation. However, if the interaction between dislocations is ignored, the structural parameters l_b and l_d of the TGB_A phase cannot be determined for chiral strengths intermediate between the lower and the upper critical chiral strengths. From an analysis which is valid close to the upper critical strength h_{c2} (where the TGB_A phase becomes unstable to the cholesteric phase), Renn and Lubensky [1] estimated that the ratio l_b/l_d increases from a minimum of about 0.96 to1.47 as the ratio K/K_2 of the splay-bend elastic constant to the twist elastic constant increases from zero to 10^4 for $\kappa_2 = 0.8$. The structural parameters l_b and l_d have been measured in the recent experiments of Navailles et al [2] on the compound 3-fluoro-4[(s)-1-methylheptyloxy]-4′-(4″-

alkoxy-$2''$,$3''$-difluorobenzoyloxy) tolane (10F2BTF01M7 for short) which has the following phase sequence: SmC*(99.7^{0}C) TGB$_A$ (102.85^{0}C) N_L^* (106.71^{0}C)N^* where N_L^* denotes the chiral line liquid phase. This TGB$_A$ phase has "commensurate" structure in which the ratio of pitch (P) over l_b is a rational number. A typical x-ray diffraction pattern is reproduced in Fig.(6.1) from the reference [2]. The pitch value P

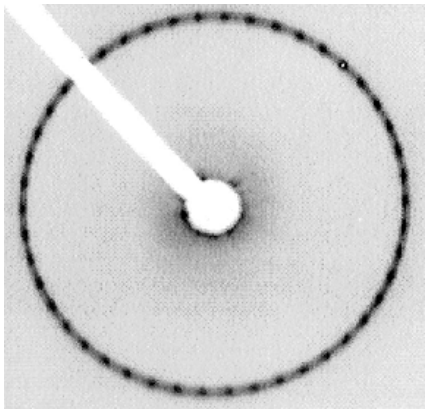

Figure 6.1: Xray diffraction pattern of an aligned TGB$_A$ sample. This pattern exhibits 46 spots equispaced along a ring and is the signature of a commensurate TGB$_A$ phase. (adapted from ref. [2]), (Temperature:101.4 ^{0}C).

in the TGB$_A$ was measured as a function of temperature by optical experiments. The ratio of P and the number of Bragg spots gives l_b at any temperature. The value of l_d was estimated using the relation $P = 2\pi l_b l_d / d$. For example, the values of l_b and l_d at a temperature of 101.4 ^{0}C are 206 $\overset{0}{A}$ and 278 $\overset{0}{A}$ respectively. The ratio l_b / l_d was found to be ~1 at 99.8 ^{0}C and reduced to ~0.7 at 101.8 ^{0}C [2,3].

In this paper we account for dislocation interactions in a systematic way to estimate l_b and l_d . While this work was in progress, Bluestein et al [3,4] presented an independent calculation for determining structural parameters of the TGB$_A$ phase. Their calculations were made in the Fourier space. On the other hand the work presented in this chapter is a direct generalisation of the Read-Shockley method for evaluating the energy of small-angle grain boundaries in solids [5]. We also present results on the temperature dependences of the structural parameters. This was not discussed by Bluestein et al [3,4].

In what follows we first calculate the elastic free energy per unit area of a twist grain boundary in type-II SmA using the linear elasticity theory. Next we calculate the Gibbs free energy of the TGB_A phase. For simplicity we consider the interactions between nearest neighbour grain boundaries only and calculate the Gibbs free energy and the structural parameters l_b and l_d. We use the mean-field dependences of ξ, λ_2 and D to calculate the temperature dependences of the structural parameters of the TGB_A liquid crystal.

In order to facilitate the evaluation of the Gibbs free energy of the TGB_A phase, we generalize the standard method of calculating the energy of topological defects to a type-II SmA liquid crystal. We first demonstrate this method for a single screw dislocation, and then use it for the energetics of pure twist grain boundaries. We note that this treatment is quite general, and can be used for the energetics of edge- as well as mixed dislocations.

6.2 Energetics of a Single Screw Dislocation

In a type–II SmA layer distortions are screened by the Frank director. For small distortions the elastic free energy density is given by [6]

$$F = \int d^3x \; f \,,$$

and

$$f = \frac{D}{2}\left(\nabla u + \overrightarrow{\delta n}\right)^2 + \frac{K_1}{2}\left(\nabla . \overrightarrow{\delta n}\right)^2 + \frac{K_2}{2}\left(\nabla \times \overrightarrow{\delta n}\right)^2 \qquad (6.1)$$

where u is the displacement field, $\overrightarrow{\delta n}$ is the deviation of the Frank director from its undistorted equilibrium value $\hat{n}_0$ (parallel to the unit vector $\hat{e}_z$ along the z- axis), and D, K_1, and K_2 are elastic constants (here we have set the twist elastic constant equal to the bend elastic constant). We write the free energy density f as

$$\begin{aligned} f = \frac{1}{2}\big[& D\nabla_i\left(u\left(\nabla_i u + \delta n_i\right)\right) - Du\nabla_i\left(\nabla_i u + \delta n_i\right) + K_1\nabla_i\left(\delta n_i \nabla_j \delta n_j\right) \\ & + K_2\varepsilon_{ijk}\nabla_j\left(\delta n_k \varepsilon_{ipq}\nabla_p \delta n_q\right) + D\delta n_i\left(\nabla_i u + \delta n_i\right) - K_1\delta n_i\left(\nabla_i \nabla_j \delta n_j\right) \\ & + K_2\delta n_i\left(\varepsilon_{ijk}\varepsilon_{kpq}\nabla_j \nabla_p \delta n_q\right) \big] \end{aligned} \qquad (6.2)$$

and treat the continuous but multivalued displacement field u for a screw dislocation as a single-valued field, which is discontinuous across a cut surface containing the dislocation line. It is important to note that in this treatment there is no topological constraint on the $\overrightarrow{\delta n}$ field. The $\overrightarrow{\delta n}$- field merely adjusts itself to lower the dislocation

energy by screening the topologically constrained displacement field. Using the Euler-Lagrange equations corresponding to the free energy in equation (6.1) we get,

$$\frac{\delta F}{\delta u} = -D\nabla.\left(\nabla u + \vec{\delta n}\right) = 0,$$
$$\frac{\delta F}{\vec{\delta n}} = D\left(\nabla u + \vec{\delta n}\right) - K_1\nabla\left(\nabla.\vec{\delta n}\right) + K_2\nabla\times\nabla\times\vec{\delta n} = 0\,. \qquad (6.3)$$

Applying Gauss's theorem, and using equation (6.2) F can be recast in the following form:

$$F = \frac{D}{2}\int_S dS_i\left(\nabla_i u + \delta n_i\right) u$$
$$= \frac{D}{2}\int_C dl\left(\nabla_i u + \delta n_i\right)\left(N^+u^+ + N^-u^-\right) L_z$$
$$= \frac{D}{2}\int dx\left(\nabla_i u + \delta n_i\right) N_i\left(u^+ - u^-\right) L_z \qquad (6.4)$$

where C is the cut line, N_i represent the components of the normal vector on the lip of the cut line (see Fig.(6.2)). $d=(u^+-u^-)$ is the magnitude of the Burgers vector, and L_Z is the length of the dislocation line.

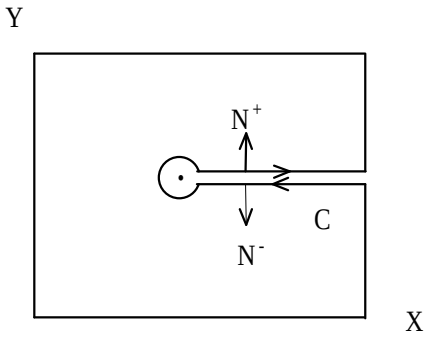

Figure 6.2: A pictorial representation of the cut surface. The dislocation line is along the z axis.

In particular, the energy per unit length for a single screw dislocation is then given by

$$\left(\frac{F}{L_z}\right) = \frac{D}{2}\int_\xi^\infty d\left(\nabla_y u + \delta n_y\right) dx, \qquad (6.5)$$

where ξ is the smectic correlation length, the screw dislocation line is along the z-axis and the cut line is along the x- axis. Here we have ignored the contribution from the dislocation core energy, which arises from the destruction of smectic order within a region of order of the smectic correlation length ξ. For a screw dislocation (dislocation line along the z – axis) at the origin the displacement field and the Frank director field are given by [6]

$$u = \frac{d}{2\pi}\varphi, \tag{6.6}$$

$$\overrightarrow{\delta n} = \frac{d}{2\pi}\left[\frac{1}{\lambda_2}K_1\left(\frac{\rho}{\lambda_2}\right) - \frac{1}{\rho}\right]\hat{e}_\phi, \tag{6.7}$$

where $\varphi = \tan^{-1}(y/x)$, $\rho = \sqrt{x^2 + y^2}$, $\hat{e}_\varphi$ is the unit vector in the φ direction, λ_2 is the twist penetration depth and $K_1(\rho/\lambda_2)$ in the modified type-II Bessel function of order one [7]. Note that the $\overrightarrow{\delta n}$- field is divergence-free. We now use these fields in equation (6.5) to evaluate the energy per unit length of a single screw dislocation:

$$\left(\frac{F}{L_z}\right)_S = -\frac{d^2 D}{4\pi}K_0\left(\frac{\xi}{\lambda_2}\right), \tag{6.8}$$

where $K_0(\xi/\lambda_2)$ is the modified type-II Bessel function of order zero. For small arguments $K_0(\xi/\lambda_2) \approx -\ln(\xi/\lambda_2)$ and we regain the standard result for the energy of a screw dislocation in strongly a type-II SmA [1, 6]

$$\left(\frac{F}{L_z}\right)_S = \frac{d^2 D}{4\pi}\ln\frac{\lambda_2}{\xi}, \tag{6.9}$$

6.3 Energetics of a Single Twist Grain Boundary

The method described above can be extended to evaluate the energy per unit area of a small-angle twist grain boundary [5]. In order to implement this we need to calculate the *u*- and the $\overrightarrow{\delta n}$ fields for a planar array of equally spaced parallel screw dislocation lines. Let us consider a grain boundary made up of screw dislocation lines parallel to $\hat{e}_z$ in the *reference lattice*, situated at $x = 0$, $y = \nu\ l_d$, where ν is an integer and l_d is the spacing between successive dislocations. Instead of directly finding the total displacement field $(u)_{TGB}$ due to the grain boundary, it is more convenient to find the local slope $(\nabla u)_{TGB}$ of the smectic layers as a function of the coordinates. For the linear elasticity theory (see equation (6.1)) the superposition principle is applicable and we merely need to add the contributions from each dislocation in the array. The displacement field is given by $u = \frac{d}{2\pi}\tan^{-1}\left(\frac{y}{x}\right)$. For a single dislocation the components of the slope of the displacement fields are given by

$$\nabla_x u = -\frac{d}{2\pi}\frac{y}{x^2+y^2}$$

$$\nabla_y u = \frac{d}{2\pi}\frac{x}{x^2+y^2}$$

For the TGB_A phase

$$\left(\nabla_x u\right)_{TGB} = \sum_{\upsilon=-\infty}^{\upsilon=\infty} -\frac{d}{2\pi}\frac{\left(y-\upsilon l_d\right)}{x^2+\left(y-\upsilon l_d\right)^2} \tag{6.10}$$

$$\left(\nabla_y u\right)_{TGB} = \sum_{\upsilon=-\infty}^{\upsilon=\infty} \frac{d}{2\pi}\frac{x}{x^2+\left(y-\upsilon l_d\right)^2} \tag{6.11}$$

We evaluate the sum in equation (6.10) by using results from complex analysis [8]:

$\sum_{\upsilon} f(\upsilon)$= - Sum of residues of [π cot(πz) *f*(z)] at all poles of *f*(z).

where $f(z)=\frac{\left(y-zl_d\right)}{x^2+\left(y-zl_d\right)^2}$. The poles of *f*(z) are at $z=\left(y\pm ix\right)\frac{1}{l_d}$. The residue at $z=\left(y+ix\right)\frac{1}{l_d}$ is given by $-\frac{\pi}{2l_d}\cot\left[\frac{\pi}{l_d}\left(y+ix\right)\right]$ and the residue at $z=\left(y-ix\right)\frac{1}{l_d}$ is given by $-\frac{\pi}{2l_d}\cot\left[\frac{\pi}{l_d}\left(y-ix\right)\right]$. Thus the sum of residues of $f(z)$ is

$$-\frac{\pi}{l_d}\frac{\sin\left(\frac{2\pi y}{l_d}\right)}{\cosh\left(\frac{2\pi x}{l_d}\right)-\cos\left(\frac{2\pi y}{l_d}\right)}. \tag{6.12a}$$

Similarly from equation (6.11) we obtain the sum of the residues as

$$-\frac{\pi}{l_d}\frac{\sinh\left(\frac{2\pi x}{l_d}\right)}{\cosh\left(\frac{2\pi x}{l_d}\right)-\cos\left(\frac{2\pi y}{l_d}\right)} \tag{6.12b}$$

Using equations (6.10), (6.11) and (6.12a), (6.12b) we get

$$\left(\nabla_x u\right)_{TGB} = -\frac{d}{2l_d}\frac{\sin\left(2\pi\ y/l_d\right)}{\cosh\left(2\pi\ x/l_d\right)-\cos\left(2\pi\ y/l_d\right)}. \tag{6.13}$$

and

$$\left(\nabla_y u\right)_{TGB} = \frac{d}{2l_d}\frac{\sinh\left(2\pi\ x/l_d\right)}{\cosh\left(2\pi\ x/l_d\right)-\cos\left(2\pi\ y/l_d\right)}. \tag{6.14}$$

It is easy to check that the dislocation lines comprising the twist grain boundary remain parallel to $\hat{e}_z$ in the direct lattice. To calculate the energy per unit area of a grain boundary we need to know the *y*- component of the $\vec{\delta n}$ field, so that the generalized version of equation (6.4) for a grain boundary can be used (see equation (6.18) below). We notice that the $\vec{\delta n}-$field for a twist grain boundary can be obtained via the Euler-Lagrange equation $\frac{\delta F}{\vec{\delta n}} = 0$, which implies

$$\nabla^2 \left(\vec{\delta n}\right)_{TGB} - \lambda_2^{-2} \left(\vec{\delta n}\right)_{TGB} = \lambda_2^{-2} \left(\nabla u\right)_{TGB} \tag{6.15}$$

We take advantage of the fact that the displacement field $\left(\nabla u\right)_{TGB}$ satisfies the Laplace equation and make the ansaz

$$\left(\delta n_y\right)_{TGB} = \left(g(x) - 1\right) \left(\nabla_y u\right)_{TGB} \tag{6.16}$$

for the particular integral of equation (6.15) to get $g(x) = e^{-|x|/\lambda_2}$. The $\left(\vec{\delta n}\right)_{TGB}$ and $\vec{Q}_y = \left\{ \left(\nabla u\right)_{TGB} + \left(\vec{\delta n}\right)_{TGB} \right\}$- fields have to satisfy the following boundary conditions:

(i) $\left(\vec{\delta n}\right)_{TGB} = 0$ at the dislocation cores, i.e., at *x=0, y=* $\nu\, l_d$, where ν is any integer, and

(ii) $\vec{Q}_y = \left\{ \left(\nabla u\right)_{TGB} + \left(\vec{\delta n}\right)_{TGB} \right\} = 0$ at $x = \pm\infty$.

To satisfy these boundary conditions we add the appropriate solution to the homogeneous version of the Euler-Langrange equation (6.15) to get

$$\vec{Q}_y = e^{-|x|/\lambda_2} \left[\left(\nabla_y u\right)_{TGB} + \frac{1}{\lambda_2} \left(|x| \left(\nabla_y u\right)_{TGB} - \frac{xd}{2l_d} \right) \right]. \tag{6.17}$$

It is now straightforward to generalise equation (6.5) to evaluate the twist grain boundary energy per unit area. With planar cut surfaces parallel to the *xz*-plane containing the dislocation lines (so that the normals to C_v are along $\pm\hat{e}_y$), the energy per unit area for the twist grain boundary is

$$f_{gb} = \lim_{L_y \to \infty} \frac{Dd}{2L_y} \sum_{v} \int_{C_v} \vec{Q}_y . \hat{e}_y dx, \tag{6.18}$$

where L_y is the length of the grain boundary along $\hat{e}_y$, and we have ignored the dislocation core energy per unit area of the grain boundary. Equation (6.18) generalizes the Read-Shockley method for calculating the energy per unit area of small-angle grain boundaries in crystals [5] to the case of small-angle grain boundaries in type-II SmA.

6.4 Interacting Twist Grain Boundaries

To estimate the structural parameters of the TGB_A phase, it is necessary to include the inter-grain boundary interactions. In what follows we numerically evaluate the nearest neighbour grain boundary interaction. This is easily done within the formulation developed above. We place parallel screw dislocations at $x = \pm l_b/2$, $y = \nu\ l_d$ in the *reference lattice* and superpose the layer displacement field $(\nabla_y u)_{TGB}$ as well as the director field component $(\delta n_y)_{TGB}$ for these two grain boundaries. We emphasize that the superposed field has the correct symmetry in the *direct lattice*: $-(\nabla_y u)_{TGB} = \pm d / l_d$ at $x = \pm\infty$. The equation (6.18) for the energy per unit area of a single grain boundary is also applicable to the case of two interacting grain boundaries, with the modification that the cut lines C_v extend from $y = \nu\ l_d,\ x = l_b/2$ to $+\infty$ and $x = -l_b/2$ to $-\infty$. The energy density for two interacting grain boundaries can be written as

$$f_{gb}^{\text{int}} = \frac{Dd}{l_b l_d}\left[\int_{\xi + l_b/2}^{\infty} Q_y\left(x + l_b/2\right)dx + \int_{-\xi - l_b/2}^{-\infty} Q_y\left(x - l_b/2\right)dx\right] \tag{6.19}$$

The chiral term favoring twist and the formation of grain boundaries in the SmA phase is given by [6]

$$F_{Ch} = -h\int d^3x\ \hat{n}.(\nabla \times \hat{n}) \tag{6.20}$$

where *h* is a *pseudoscalar* coefficient which measures the chiral strength of the liquid crystal molecules. The chiral energy per unit volume is given by

$$f_{Ch} = \frac{F_{Ch}}{V} = -hk_0 \approx -\frac{hd}{l_d l_b} \tag{6.21}$$

where k_0 is the wave vector corresponding to the twist. The total energy per unit volume is obtained by using equations (6.19) and (6.21):

$$G = f_{gb}^{\text{int}} + f_{Ch} \tag{6.22}$$

We numerically minimize the Gibbs free energy *G* as functions of l_b and l_d for different values of λ_2, ξ and *h/D*. A representative variation of the Gibbs free energy for nearest neighbour interaction calculated for $d = \xi = 38\,\overset{0}{A}$ and $\lambda_2 = 75\,\overset{0}{A}$ (i.e. $\kappa_2 = 1.97$) is shown in Fig. (6.3).

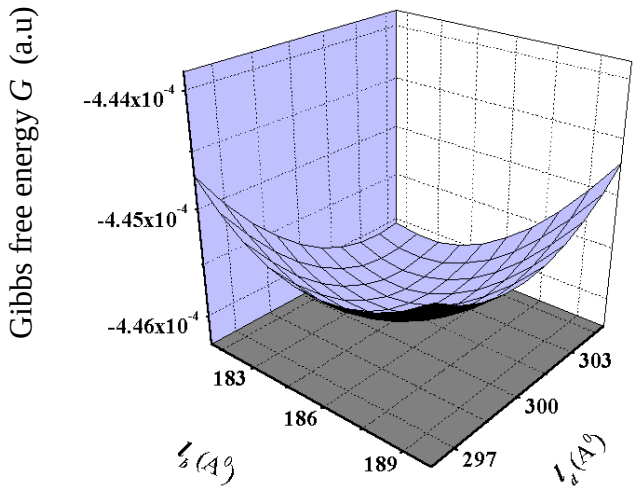

Figure 6.3: A three-dimensional plot of free energy density as a functions of l_b and l_d for $\kappa_2 = 1.97$ ($\lambda = 75\ \overset{0}{A}$, $d = \xi = 38\ \overset{0}{A}$) and $h/D = 6.5\ \overset{0}{A}$. The minimum of the energy is situated at l_b=183 $\overset{0}{A}$ and $l_d = 302\ \overset{0}{A}$.

We have calculated l_b and l_d as functions of h/D for various values of κ_2. The variations of l_b and l_d as functions of h/D are shown for κ_2 =1 in Fig.(6.4), and for κ_2 =1.44 and 1.97 in Fig.(6.5) and Fig.(6.6) respectively. We find the lower critical value of (h_{c1}/D) for different values of κ_2 at which the Gibbs free energy becomes

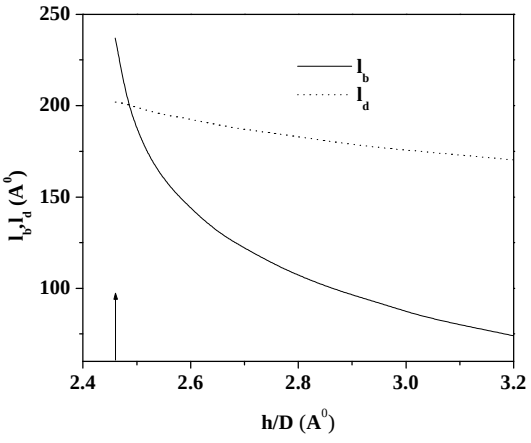

Figure 6.4: Variations of l_b and l_d as functions of h/D for $\kappa_2 = 1$ ($\lambda_2 = 38\ \overset{0}{A}$, $\xi = 38\ \overset{0}{A}$ and $d = 38\ \overset{0}{A}$). Vertical arrow denotes the lower critical value of $h_{c1}/D = 2.46$.

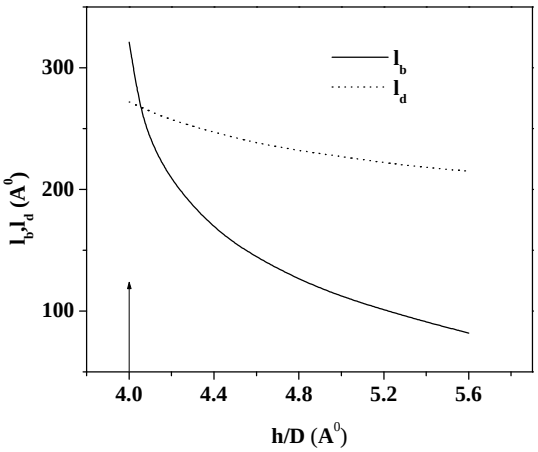

Figure 6.5: Variations of l_b and l_d as functions of *h/D* for $\kappa_2 = 1.44$ (λ_2 = 55 $\overset{0}{A}$, ξ =38 $\overset{0}{A}$ and *d* = 38 $\overset{0}{A}$). Vertical arrow denotes the lower critical value of h_{c1} / D = 4.0.

positive. In Fig.(6.4), (6.5) and (6.6) the lower critical values of h_{c1} / D are indicated by vertical arrows. We note that in each figure near h_{c1} / D the two curves intersect. Further, l_b decreases more rapidly than l_d with increasing values of *h /D*. With increasing values of κ_2 the values of h_{c1} / D also increase. Fixing the value of l_b, *h /D* also increases with κ_2 (e.g. compare Fig.(6.4), (6.5) and (6.6)) .

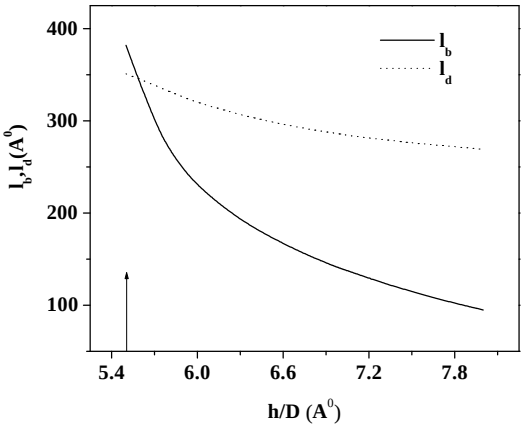

Figure 6.6: Variations of l_b and l_d as functions of *h/D* for $\kappa_2 = 1.97$ (λ_2 = 75 $\overset{0}{A}$, ξ =38 $\overset{0}{A}$ and *d* = 38 $\overset{0}{A}$). Vertical arrow denotes the lower critical value of h_{c1} / D = 5.5.

In order to find the temperature dependences of l_b and l_d we need to know the temperature dependences of the input parameters λ_2, $\xi_\perp$, h, and D. X-ray scattering studies show that $\xi_\perp \propto t^{-\nu_\perp}$ where $t = (T_{AN} - T)/T_{AN}$. $\nu_\perp$ is system–dependent, and varies between 0.45 to 0.6 [9]. In the above, T_{AN} is the SmA to TGB_A transition temperature. We have assumed that ξ and other parameters have similar dependences in the SmA and TGB_A phases. Measurements on several systems show that the *compression modulus* $B \propto t^x$, $x \approx 0.4$, whereas mean field theory predicts that $B, D \propto |\psi|^2 \propto t$, where ψ is the smectic order parameter. Further, K_2 is temperature independent, and $\lambda_2, \xi \propto t^{-0.5}$ within the mean field theory. Assuming that h is independent of temperature, calculations based on the mean field theory show that l_b decreases faster than l_d with increasing temperature. The ratio l_b / l_d as well as the pitch $P = \frac{2\pi l_b l_d}{d}$ decrease with temperature (Table-I). All these results are in accordance with the experimental trends. However, these calculations show that the stability range of the TGB_A phase is about 1^0C which is relatively small. Several experimental systems are known in which the TGB_A phase is stable over a range of 10 ^{0}C or more. Following the experimental results, even if we assume that $D \propto t^{0.5}$ there is no significant increase in the stability range of the TGB_A phase. The wide range of TGB_A phase suggests that the Ginzburg parameter κ_2 may itself be temperature dependent.

Table-I

T_{AN} -T (^{0}C)	λ ($\overset{0}{A}$)	ξ ($\overset{0}{A}$)	κ_2	h (dynes/cm)	l_b ($\overset{0}{A}$)	l_d ($\overset{0}{A}$)
1.66	75	38	1.97	0.1	345	345
1	96.5	49	1.97	0.1	70	335

In optical experiments on relatively short-pitch TGB_A systems a selective reflection band is observed [10], whereas in large-pitch systems no selective reflection is seen [11]. These apparently conflicting observations can be explained by examining the curvature of the Gibbs free energy (as a function of l_b and l_d) at its minimum. We

find that $\frac{\partial^2 G}{\partial l_d^2}$ is always greater than $\frac{\partial^2 G}{\partial l_b^2}$. Further $\frac{\partial^2 G}{\partial l_b^2}$ for *h/D*=7.1 (short-pitched system) and $\kappa_2 = 1.97$ is about 30 times that for *h/D* =5.7 (large-pitched systems). This indicates that the shallow nature of *G* as a function of l_b near its minimum may smear out the selective band for large pitched systems at finite temperatures.

6.5 Conclusions

We have used the linear elasticity theory of type-II SmA to calculate the structural parameters of the TGB_A phase. It is perhaps relevant to note that in contrast to the case of superconductors, there are two distinct kinds of vortices (edge- and screw dislocations) in the smectic-A phase. In our calculation we have ignored the edge-like fluctuations of the screw dislocation lines. We speculate that these fluctuations may give rise to long–range interactions needed to explain the possible commensurate structure of the TGB_A phase.

Further work to include interaction between all grain boundaries with a view to critically compare and contrast our method with that of Bluestein et al is desirable.

References

[1] S. R. Renn, and T.C. Lubensky, " Abrikosov Dislocation Lattice in a Model of the Cholesteric to Smectic-A Transition.," Phys. Rev. A, **38**, 2132 (1988).

[2] L. Navailles, R. Pindak, P. Barois, and H. T. Nguyen, "Structural study of the smectic-C twist grain boundary phase.," Phys. Rev. Lett. **74**, 5224 (1995).

[3] I. Bluestein, R. D. Kamein, and T.C. Lubensky, " Dislocation geometry in the TGB_A phase: linear theory.," Phys. Rev. E, **63** 061702 (2001).

[4] I. Bluestein, R. D. Kamein, " Nonlinear effects in the TGB_A phase.," Europhysics Lett. **59**, 68 (2002).

[5] N. T. Read and W. Shockley, “Dislocation models for crystal grain boundaries.,” Phys, Rev. **78**, 245 (1950).

[6] P. M. Chaikin and T. C. Lubensky, “Principle of Condenced Matter Physics.,” (Cambridge University Press, 1995).

[7] Note that the layer displacement field u has a purely topological character. We have checked that adding an analytic part (which is the solution of the Euler-Lagrange equation (6.3) with appropriate boundary conditions) to u leads to a higher energy field configuration.

[8] These sums can also be performed by using the Poisson summation formula.

[9] P. G. de Gennes and J. Prost, “The Physics of Liquid Crystals.,” 2nd ed. (Oxford Science Publications, 1993).

[10] M. Li, V. Laux, H. Nguyen, G. Sigaud, P. Barois and N. Isaert, “Blue phases and twist grain boundary phase (TGB_A and TGB_C) in a series of fluoro-substituted chiral tolane derivatives.,” Liq. Cryst. **23**, 389 (1997).

[11] L . Detre, G. Joly, N. Isaert, P. Barois, H. Nguyen and I. Dozov, “Towards a spectroscopic characterisation of twisted grain boundary structure.,” Ferroelectrics, **244**, 49 (2000).